Supramolecular organoplatinum(IV) chemistry: a nanotube structure supported by hydrogen bonds†

Richard H. W. Au, Michael C. Jennings and Richard J. Puddephatt*

Received 15th January 2009, Accepted 12th February 2009
First published as an Advance Article on the web 5th March 2009
DOI: 10.1039/b900855a

The oxidative addition of 4-$BrCH_2C_6H_4$-C(=O)NH-*t*-Bu to [$PtMe_2$(bu_2bipy)], bu_2bipy = 4,4′-di-*tert*-butyl-2,2′-bipyridine, gave [$PtBrMe_2(CH_2C_6H_4$-C(=O)NH-*t*-Bu)(bu_2bipy)], which reacted with AgX and a bridging ligand LL to give binuclear complexes [{$PtMe_2(CH_2C_6H_4$-C(=O)NH-*t*-Bu)(bu_2bipy)}$_2$(μ-LL)]X_2, LL = 1,4-pyrazine or 4,4′-bipyridine, X = BF_4 or PF_6. The complexes all take part in hydrogen bonding through either NH ··· O=C, NH ··· FB or NH ··· FP interactions and, in the case with LL = 4,4′-bipyridine, X = PF_6, a supramolecular structure containing tubes is formed.

Introduction

The synthesis of supramolecular polymers and network materials is a topical and challenging field of research, with potential applications in functional materials for sensors or molecular machines, or in catalysis.[1] The synthesis of supramolecular organometallic polymers and network materials is particularly challenging because many metal–carbon bonds are reactive towards the functional groups commonly used in supramolecular self-assembly and because the organometallic complexes often contain several functional groups, so making it difficult to predict or to engineer the supramolecular structure.[2] However, despite these challenges, the synthesis of hybrid organic-inorganic macrocycles, oligomers or polymers with organometallic units in the backbone structure, together with functional groups to allow planned self-assembly, is a rapidly developing field of research. We have previously shown that organoplatinum(IV) complexes are useful for assembling hydrogen bonding groups, and that the subsequent self-assembly can give polymers, including a double-stranded polymer and a polyrotaxane.[3] The chemistry is possible because the alkylplatinum(IV) bond is stable to air and to protic reagents, and because the oxidative addition reaction used to introduce the primary functional groups occurs selectively and under mild conditions.[4]

Organic amides have proved to be a useful functional group in self-assembly through hydrogen bonding, with relevance to folding and self-assembly of proteins in biology, and oligoamides have been designed to give supramolecular structures such as single or double helices.[5] Catenanes, rotaxanes and knots, prepared by template synthesis, have been constructed to incorporate hydrogen-bonding amide functionalities.[6] Self assembly of cyclic peptides *via* amide-amide hydrogen bonding can give supramolecular structures, most notably protein nanotubes.[7] This paper reports the synthesis of an organoplatinum(IV) complex containing an amide group, and its further functionalisation to create building blocks for self-assembly. Most interesting is the formation of a hollow tube supramolecular structure, of a type potentially useful for selective absorption of small molecules.[1]

Results and discussion

Amide groups often form strong intermolecular hydrogen bonds and this typically leads to low solubility in many organic solvents. The reagent *N*-*t*-butyl-4-bromomethylbenzamide,[8] 4-$BrCH_2C_6H_4C$(=O)NH-*t*-Bu, **1**, was found to be most suitable among several reagents tested that contain both a bromomethyl group for use in oxidative addition to platinum(II) and an amide group for hydrogen bonding. In particular, the presence of the *t*-butyl group was needed to give adequate solubility in organic solvents that were compatible with the organoplatinum complex co-reagent. There is a necessary compromise involved here, because the enhanced solubility of **1** compared to reagents with smaller alkyl substituents arises because the bulky *t*-butyl group blocks the formation of strong intermolecular hydrogen bonds. It is also expected to prevent very strong hydrogen bonding in the product complexes, and this is a potential disadvantage.

The oxidative addition of the Br–CH_2 bond of **1** to [$PtMe_2$(bu_2bipy)], **2**,[9] bu_2bipy = 4,4′-di-*t*-butyl-2,2′-bipyridine, occurred easily to give the complex [$PtBrMe_2(CH_2C_6H_4C$(=O)NH-*t*-Bu)], **3**, as shown in eqn (1).

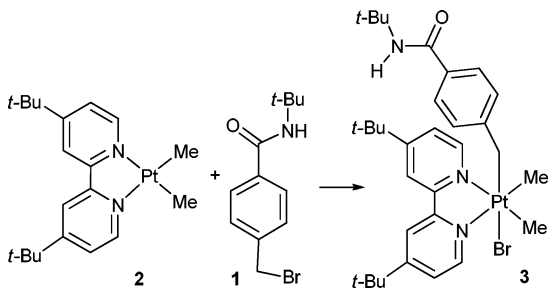

(1)

The structure of complex **3** was readily deduced from its ^{1}H NMR spectrum, which contained a single methylplatinum resonance at $\delta = 1.46$, with coupling constant ^2J(PtH) = 69 Hz, and a single Pt–CH_2 resonance at $\delta = 2.82$, with ^2J(PtH) = 96 Hz. The data show that the complex **3** is formed selectively by *trans* oxidative addition. None of the product of *cis* oxidative

Department of Chemistry, University of Western Ontario, London, Canada N6A 5B7. E-mail: pudd@uwo.ca; Fax: +1 519 661 3022; Tel: +1 519 661 2111

† CCDC reference numbers [CCDC NUMBER(S)]. For crystallographic data in CIF or other electronic format see DOI: 10.1039/b900855a

addition, which would give a more complex NMR spectrum,[3,4,10] was observed. The structure of complex **3** is shown in Fig. 1.

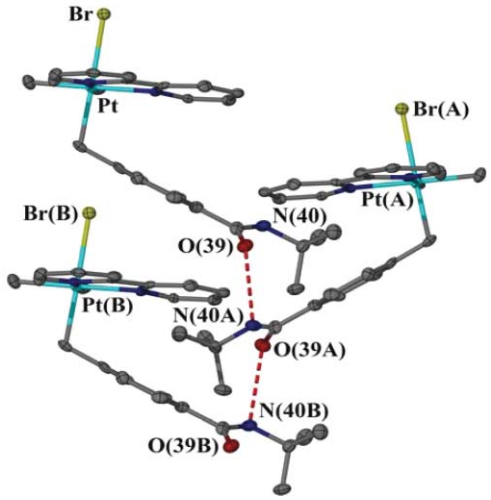

Fig. 1 The structure of complex **3**, with the *t*-butyl groups of the Bu_2bipy ligands omitted for clarity. Selected bond distances: Pt–Me = 2.02(1), 2.05(1); Pt–CH_2 = 2.10(1); Pt–N = 2.14(1), 2.16(1); Pt–Br = 2.583(1) Å. H-bond distance: N···O = 3.36(1) Å. Symmetry transformations of nearest neighbours: x, y, z; $x, -\frac{1}{2}-y, -\frac{1}{2}+z$; $x, -\frac{1}{2}-y, \frac{1}{2}+z$.

The structure (Fig. 1) confirms that **3** is formed by *trans* oxidative addition, and the benzyl group is π-stacked with one of the pyridyl groups. The amide groups are oriented as expected for formation of intermolecular NH···O=C hydrogen bonds,[1–3,5–7] but the distance O(39)···N(40A) = 3.36(1) Å is longer than the usual range of 2.5–3.2 Å in organic amides, indicating a weaker than normal hydrogen bond.[11] The very weak hydrogen bonding is attributed to the presence of the bulky *t*-butyl substituents which prevent closer approach.

Four binuclear organoplatinum(IV) complexes were prepared by reaction of the bromoplatinum complex **3** with a silver salt, $AgBF_4$ or $AgPF_6$, in the presence of a bridging ligand, pyrazine or 4,4′-bipyridyl, as shown in Scheme 1. The silver salt abstracts the bromide group from complex **3** and the bridging ligand acts as a template to assemble the two organoplatinum(IV) units. The product complexes **4** and **5** each contain two amide groups, and so have the potential to self-assemble to form polymers or network materials.

The ^{1}H NMR spectra of the complexes showed that the stereochemistry at platinum(IV) was unchanged during the reactions to give **4** and **5**. For example, the ^{1}H NMR spectrum of **4b** gave a single methylplatinum resonance at $\delta = 1.44$, with coupling constant ^2J(PtH) = 60 Hz, and a single resonance for the $PtCH_2$ protons at $\delta = 3.06$, with coupling constant ^2J(PtH) = 92 Hz. A single resonance for the pyrazine protons was observed at $\delta =$ 8.65.

The structure of complex **4a** is shown in Fig. 2. The structure of the dicationic diplatinum(IV) complex is as predicted from the NMR data. Each benzyl group is π-stacked with a pyridyl group of the adjacent bu_2bipy ligand, as in the parent complex **3**. There is a centre of symmetry at the centre of the pyrazine ligand, so the two platinum(IV) units are oriented *anti* to each other with respect to the bridging pyrazine group. There are four

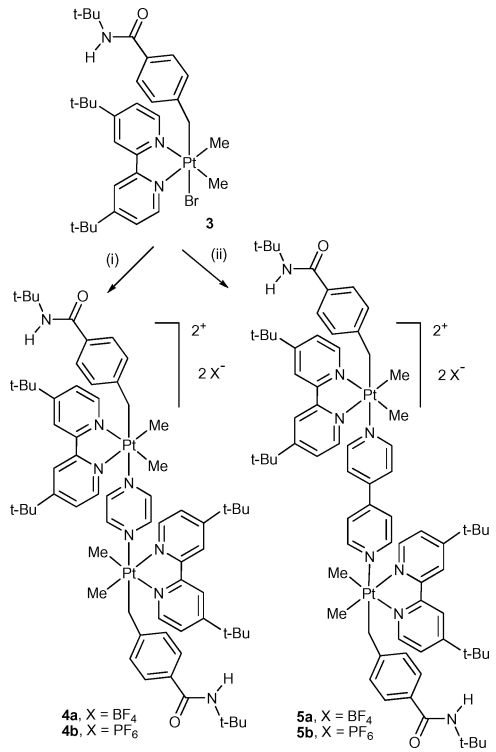

Scheme 1 Reagents: (i) AgX + pyrazine; (ii) AgX = 4,4′-bipyridine. X = BF_4 or PF_6.

methanol solvate molecules for each binuclear complex, and they and the two tetrafluoroborate anions are involved in hydrogen bonding. Each NH proton is hydrogen bonded to a tetrafluoroborate anion, which is also hydrogen bonded to a methanol molecule so giving NH···F–B–F···HOMe groupings (Fig. 2). The carbonyl groups are hydrogen bonded to the other methanol molecules to give C=O···HOMe units. The hydrogen bonding distances N(40)···F(64) = 2.920(8); N(40)···O(62) = 2.83(1); O(39)···O(81) = 2.782(8) Å are all shorter than the NH···O=C distance in complex **3**, and indicate strong hydrogen bonding.[11] Thus, it seems that the hydrogen bonding to tetrafluoroborate anions and methanol molecules is stronger than the potential amide···amide hydrogen bonding, and so complex **4a** forms only the binuclear structure shown in Fig. 2, with no long range supramolecular structure.

The structure of complex **5a** is shown in Fig. 3. The complex crystallized as a tetrahydrofuran solvate, but the THF molecules were not involved in hydrogen bonding and are not illustrated in Fig. 3. The structure is similar to that of **4a** (Fig. 2), but with a bridging 4,4′-bipyridine ligand in **5a**. There is a centre of symmetry at the centre of the 4,4′-bipyridine ligand. The benzyl groups and the platinum(IV) centres are oriented with respect to the Bu_2bipy ligands in a similar way as in complex **4a**. The NH groups in **5a** are involved in hydrogen bonding to the tetrafluoroborate anions, but the carbonyl groups are not involved in hydrogen bonding. Hence, there is no long range supramolecular structure based on the amide hydrogen bonds.

The hexafluorophosphate salts **4b** and **5b** crystallized with difficulty. However, crystals, which had the composition determined crystallographically as $[\{PtMe_2(CH_2C_6H_4C(=O)NH$-*t*-$Bu)\}_2(\mu$-4,4′-bipy$)]_3Cl[PF_6]_5\cdot 2CH_2Cl_2$, **5b′**, were finally obtained

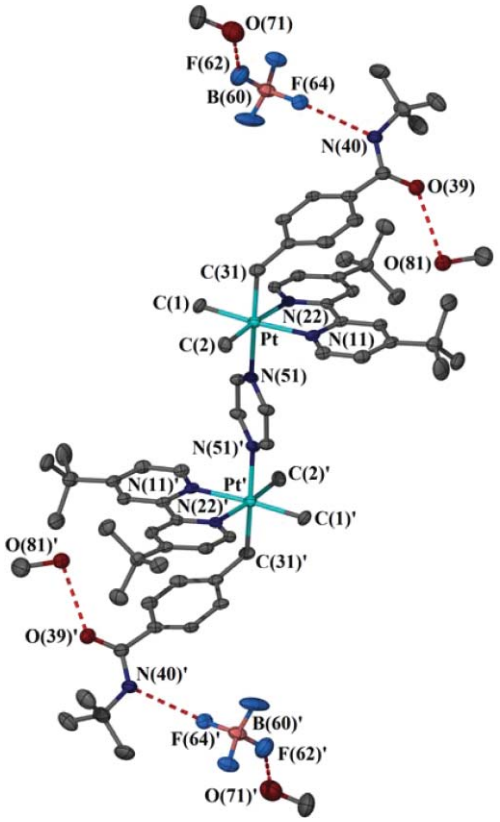

Fig. 2 The structure of binuclear pyrazine bridged complex **4a**·4MeOH. Selected bond distances: Pt–C(1) = 2.059(7); Pt–C(2) = 2.063(7); Pt–C(31) = 2.094(6); Pt–N(11) = 2.140(5); Pt–N(22) = 2.155(5); Pt–N(51) = 2.186(5) Å. Hydrogen bond distances: N(40)···F(64) = 2.920(8); N(40)···O(62) = 2.83(1); O(39)···O(81) = 2.782(8) Å.

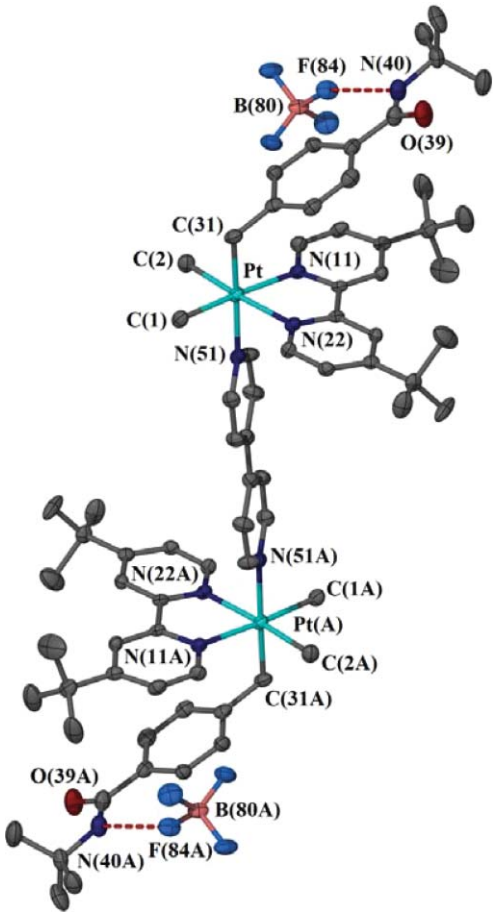

Fig. 3 The structure of binuclear 4,4′-bipyridine bridged complex **5a**·2THF. Selected bond distances: Pt–C(1) = 2.049(5); Pt–C(2) = 2.075(5); Pt–C(31) = 2.097(5); Pt–N(11) = 2.150(4); Pt–N(22) = 2.164(4); Pt–N(51) = 2.169(5) Å. Hydrogen bond distance: N(40)···F(84) = 3.125(6) Å.

from a solution of **5b**. The partial replacement of hexafluorophosphate by chloride is presumed to occur by reaction with dichloromethane solvent. The anions not involved in hydrogen bonding showed disorder but, although the accuracy of the structure is not high, the overall structure of **5b′** is reliably determined and is illustrated in Figs. 4 and 5. There are two independent binuclear dications in complex **5b′**. In one of them, containing Pt(A), there is a centre of symmetry and so the two platinum(IV) units are exactly *anti* to one another with respect to the 4,4′-bipyridine ligand, as in complex **5a** (Fig. 3). However, the second dication, containing Pt(B) and Pt(C), has no crystallographically imposed symmetry and the two platinum(IV) centres are in a staggered *syn* conformation with respect to the bridging 4,4′-bipyridine ligand, with an average torsion angle of 56° between equivalent methyl or Bu_2bipy substituents (Fig. 4). However, the more significant difference between **5b′** and **5a** is that only half of the anions (PF_6^-) are involved in hydrogen bonding to the NH groups of the amide units, and so there is a long range supramolecular structure arising from weak NH···F–P–F···HN hydrogen bonds with bridging PF_6^- ions. The two non-equivalent binuclear dications give rise to two non-equivalent supramolecular polymer chains, one containing Pt(A) centres and the other containing Pt(B) and Pt(C) centres, as illustrated in Fig. 4. Both of these polymer chains propagate in a zig-zag fashion along the *c* axis.

The most interesting feature of the structure of **5b′** is the arrangement of the polymer chains into tubes, as illustrated in Fig. 5 and 6. One of these tubes is constructed by supramolecular assembly of twelve polymer chains, four containing Pt(A) chains and eight containing Pt(B)Pt(C) chains. The hexafluorophosphate anions involved in hydrogen bonding are embedded in the chains (Fig. 4 and 5), while the free anions and resolved solvent CH_2Cl_2 molecules (not shown) are in the spaces in the lattice between the tubes. The inside of each tubes is lined with non-polar *t*-butyl groups (Fig. 6). The inner and outer diameters of the tube are ~ 16 Å and ~ 42 Å, respectively, estimated with all *t*-butyl and hydrogen atoms included. Analysis of the structure indicated that about half of the lattice space was vacant and, consistent with this surprising result, the crystal density for **5b′** was calculated to be only 0.834 g cm^{-3}, compared to a more typical value of 1.475 g cm^{-3} for complex **5a**. Analysis using the program SQUEEZE, with all solvent molecules omitted, indicated 56% void space and enough electron density (6933 e) to account for 142 CH_2Cl_2 molecules per unit cell in contrast to the 8 molecules that were located. The calculated density was then 1.26 g cm^{-3}. None of the solvent molecules inside the tubes could be located, and they are probably in a mobile, liquid-like state in those areas. The structure is robust although there are no strong secondary binding

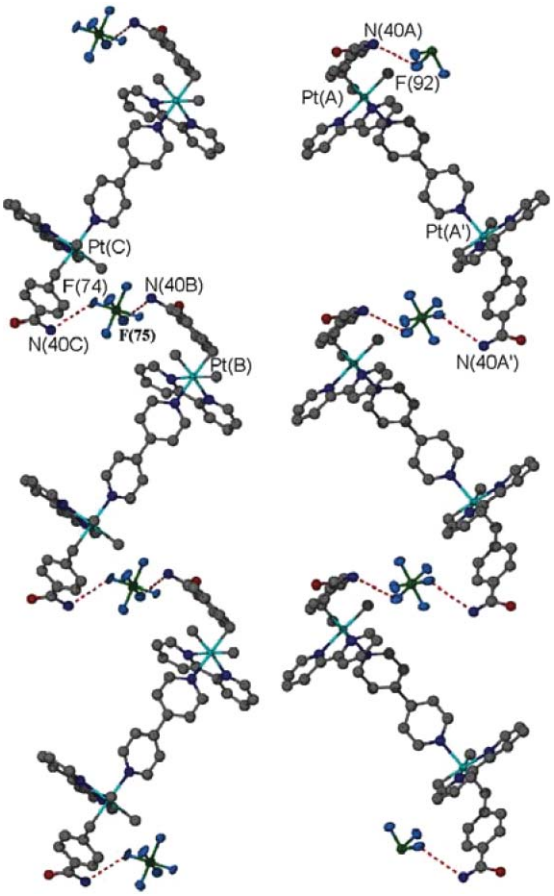

Fig. 4 The two independent supramolecular polymeric chains of binuclear complexes in **5b′**, with *t*-butyl groups omitted for clarity. Hydrogen bond distances: N(40A)···F(92) = 3.22(2); N(40B)···F(75) = 3.12(2); N(40C)···F(74) = 3.03(2) Å.

interactions between the twelve polymer chains from which the tubes are constructed. The circular tube structure, Fig. 6, has a natural strength and is not easily collapsed. The polar groups, including volatile dichloromethane molecules, held in the regions between the tubes, are evidently more tightly bound than the solvent molecules within each tube.

Conclusions

The aim of this work was to develop the supramolecular chemistry of platinum(IV)[3,4] by incorporating alkyl groups containing amide units for hydrogen bonding. The major experimental problem was that the complexes proved to have only very limited solubility when smaller amide groups were used, and so the alkyl group $CH_2C_6H_4C(=O)NH$-*t*-Bu was used to give complexes that were sufficiently soluble to be crystallized and to be characterized by NMR spectroscopy. The bulky *t*-butyl group interferes with hydrogen bonding using the adjacent NH group as H-bond donor. Intermolecular amide-amide hydrogen bonding was observed in the complex $[PtBrMe_2(CH_2C_6H_4C(=O)NH$-*t*-Bu)], **3**, eqn (1), but it was very weak (Fig. 1). Clearly, the presence of the *t*-butyl group has both an advantage (solubility) and disadvantage (limited hydrogen bonding).

In the binuclear complexes **4** and **5** (Scheme 1), amide–amide hydrogen bonding was not observed and the NH group always

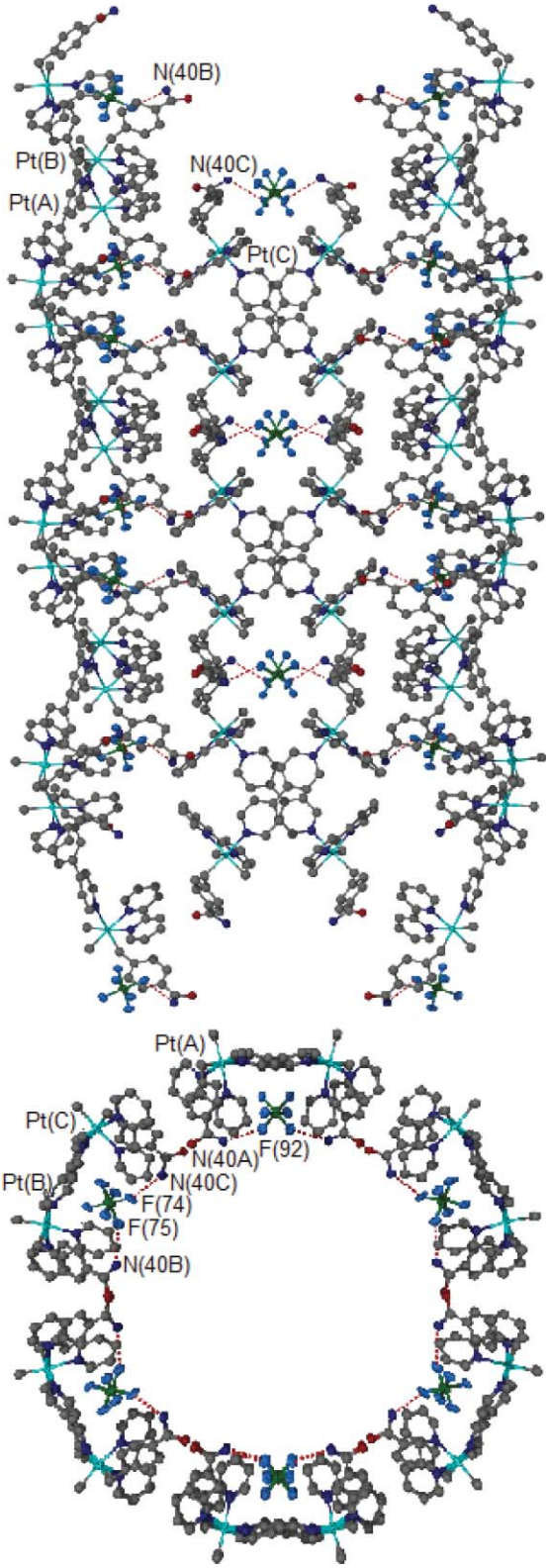

Fig. 5 Views of the hollow tube structure of complex **5b′**. The *t*-butyl groups are omitted for clarity; above, side view; below, top view.

formed a hydrogen bond to a tetrafluoroborate or hexafluorophosphate anion, presumably controlled by relative steric effects. The amide carbonyl group either formed a hydrogen bond to solvent

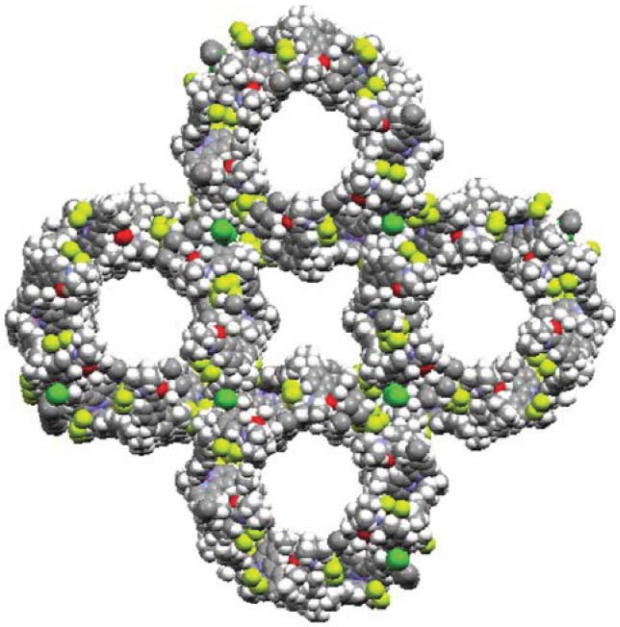

Fig. 6 A space-filling view of four adjacent tubes, and the area between them, in the structure of complex **5b′**.

(**4a**) or was not involved in hydrogen bonding (**5a**, **5b′**). The most interesting structure was the nanotube structure, assembled from twelve parallel supramolecular polymer chains, established for complex **5b′**. The structure could not have been predicted, but it does indicate the continued promise of interesting new structures in supramolecular organometallic chemistry.[1–3]

Experimental

^{1}H NMR spectra (1D and COSY to aid assignments) were recorded using a Varian Mercury 400 or a Varian Inova 400 NMR spectrometer. Exact molecular masses were determined by using a Finnigan MAT 8400 mass spectrometer. Reactions involving air-sensitive reagents were performed under a nitrogen atmosphere using standard Schlenk techniques. Solvents were HPLC grade or freshly dried, distilled and degassed prior to use when necessary. The compounds 4-$BrCH_2C_6H_4C(=O)NH$-*t*-Bu, **1**, and [$PtMe_2$(bu$_2$bipy)], **2**, were prepared using the literature methods.[8,9] Elemental analyses were performed by Guelph Chemical Laboratories LTD.

$BrCH_2$-4-C_6H_4CONH-*t*-Bu, 1[8]

NMR in $CDCl_3$: δ (^{1}H) = 1.47 [s, 9H, *t*-Bu]; 4.50 [s, 2H, $BrCH_2$]; 5.92 [s, broad, 1H, NH]; 7.44 [d, 2H, ^3J(HH) = 8 Hz, C_6H_4, H^2, H^6)]; 7.69 [d, 2H, ^3J(HH) = 8 Hz, C_6H_4, H^3, H^5]. MS: *m*/*z* calcd: 269.0415, found: 269.0418.

[$PtBrMe_2$(CH_2-4-C_6H_4CONH-*t*-Bu)(Bu$_2$bipy)], 3

A mixture of [$PtMe_2$(Bu$_2$bipy)] (50.0 mg, 0.10 mmol) and compound **1** (27.0 mg, 0.10 mmol) in acetone (10 mL) was stirred for 5 h. at room temperature. The solvent was evaporated under vacuum and the resulting solid was washed with water and then pentane. The product was isolated as a yellow solid, which was dried *in vacuo*. Yield: 94% (71.8 mg). It was recrystallized from acetone/pentane. NMR in CD_2Cl_2: δ (^{1}H) = 1.35 [s, 9H, *t*-Bu]; 1.42 [s, 18H, bipy-Bu]; 1.44 [s, 6H, ^2J(PtH) = 69 Hz, PtMe]; 2.82 [s, 2H, ^2J(PtH) = 96 Hz, $PtCH_2$]; 5.68 [s, 1H, NH]; 6.34 [d, 2H, ^3J(HH) = 8 Hz, ^4J(PtH) = 19 Hz, C_6H_4, H^2, H^6]; 6.94 [d, 2H, ^3J(HH) = 8 Hz, C_6H_4, H^3, H^5]; 7.47 [dd, 2H, ^3J(HH) = 6 Hz, ^4J(HH) = 2 Hz, bipy, H^5]; 7.97 [d, 2H, ^4J(HH) = 2 Hz, bipy, H^3]; 8.52 [d, 2H, ^3J(HH) = 6 Hz, ^3J(PtH) = 19 Hz, bipy, H^6]. Anal. calcd for $C_{32}H_{46}BrN_3OPt$: C 50.33, H 6.07, N 5.50. Found: C 49.94, H 5.76, N 5.42%.

[{$PtMe_2$(CH_2-4-C_6H_4CONH-*t*-Bu)(Bu$_2$bipy)}$_2$(μ-pyrazine)][BF_4]$_2$, 4a

A solution of $AgBF_4$ (21.1 mg, 0.1085 mmol) in acetone (5 mL) was added dropwise to complex **3** (84.5 mg, 0.1085 mmol) in acetone (15 mL) and allowed to stir for 1 h. AgBr precipitated and the mixture was filtered through Celite into a solution of pyrazine (4.3 mg, 0.05425 mmol). After 12 h of stirring at room temperature, the solvent was evaporated and the product was recrystallized from CH_2Cl_2/pentane to give a pale yellow solid. Yield: 92% (80.8 mg). NMR in CD_2Cl_2: δ (^{1}H) = 1.37 [s, 18H, *t*-Bu]; 1.43 [s, 36H, bipy-Bu]; 1.44 [s, 12H, ^2J(PtH) = 64 Hz, PtMe]; 3.06 [s, 4H, ^2J(PtH) = 96 Hz, $PtCH_2$]; 5.86 [s, 2H, NH]; 6.40 [d, 4H, ^3J(HH) = 8 Hz, ^4J(PtH) = 17 Hz, C_6H_4, H^2, H^6]; 7.03 [d, 4H, ^3J(HH) = 8 Hz, C_6H_4, H^3, H^5]; 7.68 [dd, 4H, ^3J(HH) = 6 Hz, ^4J(HH) = 2 Hz, bipy, H^5]; 7.97 [d, 2H, ^4J(HH) = 2 Hz, bipy, H^3]; 8.59 [d, 4H, ^3J(HH) = 6 Hz, ^3J(PtH) = 19 Hz, bipy, H^6]; 8.65 [s, 4H, μ-pyz]. Anal. calcd. for $C_{68}H_{96}B_2F_8N_8O_2Pt_2$: C 50.38, H 5.97, N 6.91. Found: C 50.25, H 6.20, N 7.16%.

[{$PtMe_2$(CH_2-4-C_6H_4CONH-*t*-Bu)(Bu$_2$bipy)}$_2$(μ-pyz)][PF_6]$_2$, 4b

This was prepared similarly from complex **3** (84.5 mg, 0.1085 mmol), $AgPF_6$ (27.4 mg, 0.1085 mmol) and pyrazine (4.3 mg, 0.05425 mmol). A pale yellow solid was produced. Yield: 90% (84.8 mg). NMR in CD_2Cl_2: δ (^{1}H) = 1.35 [s, 18H, *t*-Bu]; 1.43 [s, 36H, bipy-Bu]; 1.44 [s, 12H, ^2J(PtH) = 60 Hz, PtMe]; 3.06 [s, 4H, ^2J(PtH) = 92 Hz, $PtCH_2$]; 5.76 [s, 2H, NH]; 6.40 [d, 4H, ^3J(HH) = 8 Hz, ^4J(PtH) = 17 Hz, C_6H_4, H^2, H^6]; 7.02 [d, 4H, ^3J(HH) = 8 Hz, C_6H_4, H^3, H^5]; 7.67 [dd, 4H, ^3J(HH) = 6 Hz, ^4J(HH) = 2 Hz, bipy, H^5]; 8.03 [d, 2H, ^4J(HH) = 2 Hz, bipy, H^3]; 8.56 [d, 4H, ^3J(HH) = 6 Hz, ^3J(PtH) = 19 Hz, bipy, H^6]; 8.65 [s, 4H, μ-pyz]. Anal. calcd for $C_{68}H_{96}F_{12}N_8O_2P_2Pt_2$: C 47.00, H 5.57, N 6.45. Found: C 46.90, H 5.28, N 6.72%.

[{$PtMe_2$(CH_2-4-C_6H_4CONH-*t*-Bu)(Bu$_2$bipy)}$_2$(μ-4,4′-bipy)][BF_4]$_2$, 5a

This was prepared similarly from complex **3** (7.8 mg, 0.10 mmol), $AgBF_4$ (19.5 mg, 0.10 mmol) and 4,4′-bipyridyl (7.8 mg, 0.050 mmol). A pale yellow solid was produced. Yield: 90% (76.4 mg). NMR in CD_2Cl_2: δ (^{1}H) = 1.36 [s, 18H, *t*-Bu]; 1.39 [s, 36H, bipy-Bu]; 1.41 [s, 12H, ^2J(PtH) = 66 Hz, PtMe]; 2.95 [s, 4H, ^2J(PtH) = 93 Hz, $PtCH_2$]; 5.76 [s, 2H, NH]; 6.35 [d, 4H, ^3J(HH) = 8 Hz, ^4J(PtH) = 17 Hz, C_6H_4, H^2, H^6]; 6.98 [d, 4H, ^3J(HH) = 8 Hz, C_6H_4, H^3, H^5]; 7.57 [d, 4H, ^3J(HH) = 6 Hz, μ-bipy, H^3, H^5]; 7.63 [dd, 4H, ^3J(HH) = 6 Hz, ^4J(HH) = 2 Hz, bipy, H^5]; 7.96 [d, 2H, ^4J(HH) = 2 Hz, bipy, H^3]; 8.16 [d, 4H, ^3J(HH) = 6 Hz, ^3J(PtH) = 19 Hz, bipy, H^6]; 8.58 [d, 4H, ^3J(HH) = 6 Hz, ^3J(PtH) = 18 Hz,

Table 1 Crystal data and structure refinement

	3	**4a**·4MeOH	**5a**·2THF	**5b′**·CH_2Cl_2
Formula	$C_{32}H_{46}BrN_3OPt$	$C_{72}H_{112}B_2F_8$- $N_6O_6Pt_2$	$C_{82}H_{116}B_2F_8N_8O_4Pt_2$	$C_{222}H_{300}ClF_{30}N_{24}O_6P_5Pt_6$
FW	763.72	1749.50	1841.63	5331.70
T/K	150(2)	150(2)	150(2)	150(2)
Crystal system	Monoclinic	Monoclinic	Monoclinic	Tetragonal
Space group	$P2_1/c$	$P2_1/n$	$P2_1/n$	$P\bar{4}n2$
a/Å	20.9830(8)	16.9121(9)	13.2476(3)	50.993(2)
b/Å	14.4635(5)	11.2195(6)	15.2782(4)	50.993(2)
c/Å	10.5574(5)	21.758(1)	20.4940(4)	16.8394(5)
α/°	90	90	90	90
β/°	92.691(2)	96.689(2)	90.757(2)	90
γ/°	90	90	90	90
V/Å^3	3200.5(2)	4124.7(4)	4147.6(2)	4378.7(2)
Z	4	2	2	4
D_{calcd}/Mg m^{-3}	1.585	1.409	1.475	0.809
μ/mm^{-1}	5.660	3.456	3.439	1.978
F(000)	1520	1772	1868	10712
R_1, wR_2	0.062, 0.163	0.046, 0.120	0.038, 0.092	0.0953, 0.121

μ-bipy, H^2, H^6]. Anal. calcd for $C_{74}H_{100}B_2F_8N_8O_2Pt_2$: C 52.36, H 5.94, N 6.60. Found: C 51.96, H 5.94, N 6.17%.

[{$PtMe_2(CH_2$-4-C_6H_4CONH-*t*-Bu)(Bu_2bipy)}$_2$(μ-4,4′-bipy)][PF_6]$_2$, 5b

This was prepared similarly from complex **3** (7.8 mg, 0.10 mmol), $AgPF_6$ (25.3 mg, 0.10 mmol) and 4,4′-bipyridyl (7.8 mg, 0.050 mmol). A pale yellow solid was produced. Yield: 88% (79.8 mg). NMR in CD_2Cl_2: δ (^{1}H) = 1.36 [s, 18H, *t*-Bu]; 1.39 [s, 36H, bipy-Bu], 1.41 [s, 12H, ^2J(PtH) = 68 Hz, PtMe]; 2.96 [s, 4H, ^2J(PtH) = 94 Hz, $PtCH_2$]; 5.71 [s, 2H, NH]; 6.36 [d, 4H, ^3J(HH) = 8 Hz, ^4J(PtH) = 17 Hz, C_6H_4, H^2, H^6]; 6.98 [d, 4H, ^3J(HH) = 8 Hz, C_6H_4, H^3, H^5]; 7.50 [d, 4H, ^3J(HH) = 6 Hz, μ-bipy, H^3, H^5]; 7.62 [dd, 4H, ^3J(HH) = 6 Hz, ^4J(HH) = 2 Hz, bipy, H^5]; 7.97 [d, 2H, ^4J(HH) = 2 Hz, bipy, H^3]; 8.12 [d, 4H, ^3J(HH) = 6 Hz, ^3J(PtH) = 18 Hz, bipy, H^6]; 8.54 [d, 4H, ^3J(HH) = 6 Hz, ^3J(PtH) = 16 Hz, μ-bipy, H^2, H^6]. Anal. calcd for $C_{74}H_{100}F_{12}N_8O_2P_2Pt_2$: C 49.00, H 5.56, N 6.18. Found: C 49.28, H 5.66, N 6.28%.

X-Ray structure determinations

A crystal was mounted on a glass fibre. Data were collected using a Nonius-Kappa CCD diffractometer using COLLECT (Nonius, B.V. 1997–2002) software. The unit cell parameters were calculated and refined from the full data set. Crystal cell refinement and data reduction was carried out using the HKL2000 DENZO-SMN (Otwinowski & Minor, 1997). The absorption correction was applied using HKL2000 DENZO-SMN (SCALEPACK). The SHELXTL/PC V6.14 for Windows NT (Sheldrick, G.M., 2001) program package was used to solve the structure by direct methods. Subsequent difference Fourier syntheses allowed the remaining atoms to be located. All non-hydrogen atoms were refined with anisotropic thermal parameters. The hydrogen atom positions were calculated geometrically and were included as riding on their respective carbon, nitrogen and oxygen atoms. All thermal ellipsoid diagrams are shown at 35% probability except for **5b′**, which is modelled at 20%. Details of the data collection and refinement are given in Table 1. Brief comments on unusual features are given below.

[$PtBrMe_2(CH_2$-4-C_6H_4CONH-*t*-Bu)(Bu_2bipy)], 3

Crystals were grown by slow diffusion of pentane into an acetone solution.

[{$PtMe_2(CH_2$-4-C_6H_4CONH-*t*-Bu)(Bu_2bipy)}$_2$(μ-pyrazine)][BF_4]$_2$·4MeOH, 4a·4MeOH

Crystals were grown by slow evaporation of a solution of **4a** in CH_2Cl_2–MeOH.

[{$PtMe_2(CH_2$-4-C_6H_4CONH-*t*-Bu)(bu$_2$bipy)}$_2$(μ-4,4′-bipy)][BF_4]$_2$·2THF, 5a·2THF

Crystals were grown from a solution of **5a** in THF by slow diffusion of pentane. One of the *tert*-butyl groups showed some disorder and was modelled at 50/50 occupancy.

[{$PtMe_2(CH_2C_6H_4C$(=O)NH-*t*-Bu)}$_2$(μ-4,4′-bipy)]$_3$Cl[PF_6]$_5$·CH_2Cl_2, 5b′

Crystals were grown by slow diffusion of hexane into a solution of **5b** in CH_2Cl_2. The structure is of limited accuracy and all carbon atoms were treated isotropically, with heavier atoms treated anisotropically. Several constraints and restraints were applied to allow for unresolved disorder. One dichloromethane solvate molecule was located. Treatment with SQUEEZE indicated 56% void space. No solvent molecules were located in that area, but SQUEEZE indicated the presence of disordered solvent. The calculated density was 1.26 g cm^{-3} including all electron density, 0.834 g cm^{-3} including just the ordered CH_2Cl_2, and 0.809 g cm^{-3} excluding all solvent.

Acknowledgements

We thank the NSERC of Canada for financial support of this work.

Notes and references

1 J. M. Lehn, *Supramolecular Chemistry: Concepts and Perspectives*, Wiley-VCH, Weinheim, 1995; J. W. Steed, and J. L. Atwood, *Supramolecular Chemistsry*, VCH, New York, 2000; A. Y. Robin and K. M. Fromm, *Coord. Chem. Rev.*, 2006, **250**, 2127; R. Hoogenboom and U. S. Schubert, *Chem. Soc. Rev.*, 2006, **35**, 622; I. G. Georgiev and L. R. MacGillivray, *Chem. Soc. Rev.*, 2007, **36**, 1239; A. J. Wilson, *Soft Matter*, 2007, **3**, 409; C. L. Chen, B. S. Kang and C. Y. Su, *Aust. J. Chem.*, 2006, **59**, 3; B. Wang, A. P. Cote, H. Furukawa, M. O'Keeffe and O. M. Yaghi, *Nature*, 2008, **453**, 207.

2 D. Braga and F. Grepioni, *Coord. Chem. Rev.*, 1999, **183**, 19; J. C. Mareque Rivas and L. Brammer, *Coord. Chem. Rev.*, 1999, **183**, 43; I. Haiduc, and F. T. Edelmann, *Supramolecular Organometallic Chemistry*, Wiley-VCH, Weinheim, 1999; A. Laguna, *Modern Supramolecular Gold Chemistry*, Wiley-VCH, Weinheim, 2008.

3 C. S. A. Fraser, H. A. Jenkins, M. C. Jennings and R. J. Puddephatt, *Organometallics*, 2000, **19**, 1635; C. S. A. Fraser, M. C. Jennings and R. J. Puddephatt, *Chem. Commun.*, 2001, 1310; C. S. A. Fraser, M. C. Jennings and R. J. Puddephatt, *Chem. Commun.*, 2002, 1224; C. S. A. Fraser, D. J. Eisler and R. J. Puddephatt, *Polyhedron*, 2005, **25**, 266.

4 *Comprehensive Organometallic Chemistry III*, ed. A. J. Canty, Elsevier, Amsterdam, vol. 8, 2007(*a*) A. Capape, M. Crespo, J. Granell, M. Font-Bardia and X. Solans, *Dalton Trans.*, 2007, 2030; E. Hager, A. H. S. Clayton, M. M. Mogorosi and J. R. Moss, *Coord. Chem. Rev.*, 2008, **252**, 1668; M. Rashidi and B. Momemi, *J. Organomet. Chem.*, 1999, **574**, 286; D. Song, W. L. Jia and S. Wang, *Organometallics*, 2004, **23**, 1194; R. P. Hughes, R. B. Laritchev, L. N. Zakharov and A. L. Rheingold, *Organometallics*, 2005, **24**, 4845; A. J. Canty, R. P. Watson, S. S. Karpiniec, T. Rodemann, M. G. Gardiner and R. C. Jones, *Organometallics*, 2008, **27**, 3203; P. K. Monaghan and R. J. Puddephatt, *Dalton Trans.*, 1988, 595.

5 C. Dolain, V. Maurizot and I. Huc, *Angew. Chem., Int. Ed.*, 2003, **42**, 2738; J. T. Ernst, J. Becerril, H. S. Park, H. Yin and A. D. Hamilton, *Angew. Chem., Int. Ed.*, 2003, **42**, 535.

6 F. G. Gatti, D. A. Leigh, S. A. Nepogodiev, A. M. Z. Slawin, S. J. Teat and J. K. Y. Wong, *J. Am. Chem. Soc.*, 2001, **123**, 5983.

7 J. D. Hartgerink, T. D. Clark and M. R. Ghadiri, *Chem.–Eur. J.*, 1998, **4**, 1367.

8 K. L. Reddy, *Tet. Lett.*, 2003, **44**, 1453; R. W. Hartmann, M. Reichert and S. Göhring, *Eur. J. Med. Chem.*, 1994, **29**, 807.

9 J. D. Scott and R. J. Puddephatt, *Organometallics*, 1983, **2**, 1643; S. Achar, J. D. Scott, J. J. Vittal and R. J. Puddephatt, *Organometallics*, 1993, **12**, 4592.

10 M. C. Janzen, H. A. Jenkins, M. C. Jennings, L. M. Rendina and R. J. Puddephatt, *Organometallics*, 2002, **21**, 1257; L. M. Rendina and R. J. Puddephatt, *Chem. Rev.*, 1997, **97**, 1735.

11 G. R. Desiraju and T. Steiner, *The Weak Hydrogen Bond*, Oxford Science Publication, Oxford, 1999; G. A. Jeffrey, *An Introduction to Hydrogen Bonding*, Oxford University Press, Oxford, 1997.